AIAA AVIATION Forum
5-9 June 2017, Denver, Colorado
47th AIAA Thermophysics Conference

10.2514/6.2017-3163

Master equation simulation of O_2–N_2 collisions on an ab-initio potential energy surface

Daniil A. Andrienko*

Iain D. Boyd †

Department of Aerospace Engineering, University of Michigan, Ann Arbor, MI, 48109

Simulation of vibrational energy transfer in O_2–N_2 collisions is conducted using the quasiclassical trajectory method on an accurate potential energy surface. State-resolved rate coefficients are obtained for the O_2 and N_2 vibrational ladders at temperatures between 8000 and 15,000 K. A system of master equations is constructed using the new dataset in order to simulate nonequilibrium conditions observed in shock flows. The relaxation time derived from a solution of the master equations is in good agreement with the Millikan and White correlation at lower temperatures with an increasing discrepancy toward the translational temperature of 15,000 K. At the same time, the master equation relaxation time is similar to that derived under the assumption of a two-state system. This observation suggests that the multiquantum vibrational energy transfer in O_2–N_2 may be less efficient compared to that in a chemically reactive molecule-atom system.

Nomenclature

v, w	initial vibrational states of O_2 and N_2
v', w'	final vibrational states of O_2 and N_2
$\Delta v = v' - v$	O_2 vibrational quantum jump
$\Delta w = w' - w$	N_2 vibrational quantum jump
K	rate coefficient of bound-bound transition, cm^3/s
T, T_r, T_v	translational, rotational and vibrational temperatures
$v, w \rightarrow v', w'$	transition from $O_2(v)$ and $N_2(w)$ to $O_2(v')$ and $N_2(w')$
$K_{v \rightarrow v-1}$	rate coefficient of $O_2(v)$ monoquantum deactivation, cm^3/s
$p\tau_{1 \rightarrow 0}$	relaxation time, derived from $K_{1 \rightarrow 0}$ rate coefficient , atm-s
$K_{v,rem}$	removal rate coefficient, $K_{v,rem} = \sum_{v' \neq v} K_{v \rightarrow v'}$, cm^3/s

I. Introduction

Simulation of molecule-atom and molecule-molecule collisions from first principles is a vital activity in hypersonic aerothermochemistry since it can provide an increased level of accuracy when simulating high temperature flows with a degree of chemical and thermal nonequilibrium. The initial capacity for such research was formed by the ever-increasing computational power such that statistical methods became tractable as well as by the variety of potential energy surfaces (PES), developed for studies of low temperature kinetics in the upper atmosphere.[1–4]

While a large amount of previous work regarding the nonequilibrium processes in high temperature gases has concentrated on the state-resolved chemistry of nitrogen[5–9] and nitric oxide[10–14] due to the importance of these species in re-entry and combustion problems, thermochemistry of oxygen has received less attention. This is due to the fact that the atmosphere contains only 0.2 molar fraction of oxygen, and it dissociates

*Postdoctoral research fellow, Department of Aerospace Engineering, University of Michigan, 1320 Beal Ave
†James E. Knott Professor, Department of Aerospace Engineering, University of Michigan, 1320 Beal Ave

easily under harsh re-entry conditions. However, recent success and setbacks of hypersonic flight projects have directed research in the study of oxygen nonequilibrium thermalization at lower speeds that correspond to the flight conditions of air-breathing hypersonic vehicles.

For diatomic oxygen, the most relevant collisions in terms of rovibrational relaxation and dissociation are observed with O, O_2 and, most importantly, with N_2. Currently, only the first type of these collisions has been studied in detail. For the O_2–O system, a number of PESs[15–18] of different fidelity are available due to the ability of O_3 to absorb harmful ultra-violet radiation.[19] High-temperature kinetics of O_2–O collisions received special attention recently due to anomalously high rate coefficients (RC) of vibrational transitions.[20,21] This phenomenon is associated with the small potential barrier in the entrance/exit channel of the O_2–O interaction.

The study of collisions of molecular oxygen with other diatomic air species is limited to low temperatures (say, 1000 K). There are a number of O_2–O_2[1,2,22] and O_2–N_2[3,23] PESs, however they are designed only for low energy collisions. In many cases, these PESs are either limited to a rigid rotor approximation, or utilize empirical data to approximate the intermolecular forces, or do not describe the potential energy in bond-breaking collisions. Nevertheless, the semi- and quasi-classical calculations, conducted on these PESs, showed good agreement with measurements in the rates of vibration-translation and vibration-vibration energy transfer between diatomic species at room temperatures.[24] The interest in such kinetic models is dictated by the disagreement in theoretical and experimental predictions of ozone formation rates,[4] probably due to some shadow mechanisms involving vibrationally excited O_2.[25,26]

Only recently the investigation of bimolecular collisions at higher temperatures received attention. Six-dimensional N_4 PESs based on accurate quantum calculations were developed at the NASA Ames Research Center[27] and at the University of Minnesota.[28] More interesting, in the context of the present paper, is the recent global O_2N_2 PES by Varga et al.[29] However, full-blown quasi-classical trajectory (QCT) simulations including all rovibrational states appears to be computationally intractable using these high-quality PESs. One of the possible ways to overcome this difficulty is the direct molecular simulation method, developed by Koura.[30] While this approach makes it possible to obtain the average macroscopic parameters of thermally and chemically nonequilibrium gas mixtures, such as vibrational and rotational relaxation times and the quasi-steady state (QSS) dissociation RC, this method does not allow extraction of the state-specific transition RCs that are typically required for further kinetic modeling in fluid dynamic codes and experiments.

The present paper features the QCT calculations of bound-bound rate coefficients, conducted on the new O_2N_2 PES and compares this data with the results of other available models. In Section II, the governing equations are given. Section III presents the master equation simulation of the O_2–N_2 system. Conclusions are drawn in Section IV.

II. Computational approach

The quasi-classical trajectory method presents a compromise between the accuracy of statistical simulation of trajectory propagation and its cost. There are only a few alternatives to the QCT method when attempting to resolve all possible rovibrational state-specific cross sections at high kinetic energies, i.e. when inelastic collisions occur frequently, providing small statistical uncertainty of results. The QCT method yields 12 and 18 Hamiltonian equations when applied to molecular systems with three (atom-diatom) and six (diatom-diatom) degrees of freedom. These numbers can be reduced to 8 and 14 by recognizing that the total energy and total angular momenta are conserved. On the other hand, the semi-classical (SC) coupled approach, proposed by Billing,[31] involves additional time-dependent Schröedinger equations, whose number is proportional to the number of vibrational states involved in a trajectory simulation. At hypersonic temperatures, when the population of all vibrational states must be captured, such a method becomes computationally intractable.

In the present work, the simulation of molecule-molecule collisions is conducted using an in-house four-body QCT code. An extensive overview of three- and four-body QCT methods is given elsewhere.[32] The present paper concentrates on kinetic models of hypersonic flows and provides discussion on utilization of the QCT data. The primary tool for analysis of state-specific RCs, generated by the QCT method, is the system of master equations. The general appearance of the master equation for collisions of molecular oxygen with molecular nitrogen includes the bound-bound and bound-free processes and is given by Eq. (1)

$$\frac{dn_v}{dt} = \sum_{v' \neq v, w', w} K_{v', w' \to v, w} n_{w'} n_{v'} - \sum_{v \neq v', w, w'} K_{v, w \to v', w'} n_w n_v - \quad (1)$$
$$- \sum_{w, w'} D_{v, w \to w'} n_v n_w + \sum_{w, w'} R_{w' \to v, w} n_x^2 n_{w'}, \quad v, v' = 1...N_v, w, w' = 1...N_w,$$

where n_v is the population of the v vibrational state, $K_{v',w' \to v,w}$ is the RC of reaction of $O_2\,(v')$ and $N_2\,(w')$ with the production of two molecular species in the v and w vibrational states, respectively. The RC of the reverse reaction is denoted as $K_{v,w \to v',w'}$. n_x is the number density of the dissociation projectile, $D_{(v,w) \to w'}$ and $R_{w' \to (v,w)}$ are the state-specific dissociation and recombination rate coefficients of the v state in collision with the $N_2(w)$ state with the production of $N_2(w')$, N_v denotes the total number of vibrational states. The master equation for $N_2\,(w)$ is similar to Eq. (1) with only the replacement of v to w, v' to w' and vice versa. Due to complexity of Eq. 1, the present paper considers only bound-bound transitions in the master equation, i.e. only first two terms in the right hand side.

Equation (1) describes the relaxation of molecular nitrogen and oxygen. In the present work the study of relaxation is considered only in an ideal heat bath. Initial conditions must be provided for the system of equations (1). Since the master equation simulation contains two molecules as reactants, initial conditions can be specified for each of them individually. In all simulations, the initial rotational temperature is set to the translational temperature. When vibrational relaxation is studied, the initial temperature of oxygen and nitrogen is set to either 100 K or to an equilibrium translational temperature, as specified. The first choice of the initial T_v corresponds to the strong nonequilibrium conditions, while the second choice indicates that the given molecular species is in thermal equilibrium. The initial population of the vibrational ladder is calculated from the Boltzmann distribution at specified initial vibrational temperature. Although the production of nitric oxide is observed by means of the QCT method in the range of studied temperatures, the NO formation is of secondary importance for the thermal relaxation of O_2 and N_2 and, hence, is artificially excluded from the master equation simulation. To do so, the RCs of NO formation are set to zero and the master equations for the NO vibrational ladder are excluded from the system (1). The principle of detailed balance is invoked to generate rates of endothermic transitions, in order to reduce the statistical error of the QCT method.

The system of master equations is a convenient tool for the analysis of designated energy transfer mechanisms. Since the rate coefficients between vibrational states are of primary importance for O_2 and N_2 relaxation, in the present work, the result of O_2–N_2 collisions are divided into several categories. First, vibration-translation (VT) and vibration-vibration (VV) types of collisions are described by Eqs. (2)-(3) and by Eqs. (4)-(5), respectively:

$$O_2\,(v) + N_2\,(w) \to O_2\,(v - \Delta v) + N_2\,(w) \quad (2)$$

$$O_2\,(v) + N_2\,(w) \to O_2\,(v) + N_2\,(w - \Delta w) \quad (3)$$

$$O_2\,(v) + N_2\,(w) \to O_2\,(v - \Delta v) + N_2\,(w + \Delta w) \quad (4)$$

$$O_2\,(v) + N_2\,(w) \to O_2\,(v + \Delta v) + N_2\,(w - \Delta w) \quad (5)$$

The approach for obtaining rate coefficients for reactions Eqs. (2) - (5) from the database of cross sections was described previously elsewhere.[33] The e-folding method by Park[34] is adopted to extract the vibrational relaxation time from the temporal evolution of O_2 and N_2 vibrational energy. This method is adopted throughout the paper unless stated otherwise. A simpler approach to obtain the vibrational relaxation time is based on the rate coefficient of a monoquantum deactivation from the first excited vibrational state.[35] This approach is adopted in the present paper as an alternative to the e-folding method.

III. Results

The interaction of O_2 with molecular nitrogen is of great importance in hypersonic thermochemistry due to the large difference in the dissociation energy of these species. There are several PESs in the literature that describe the N_2O_2 system. One of the first N_2O_2 PESs was proposed by Aquilanti et al.[3] for studying rigid molecules in their ground vibrational state. This PES was designed specifically for methods of molecular dynamics for conditions in the upper atmosphere, however it has a little use for aerothermodynamics. Bartolomei et al.[36] recently published an improved *ab-initio* PES with similar restrictions.

The vibration-translation (VT) and vibration-vibration (VV) energy transfer was studied by a semi-classical coupled method by Billing on an empirical PES in the range of temperatures between 250 and 1000 K.[23] Recently, Garcia et al.[37,38] reported VT and VV RCs using an improved PES for selected vibrational states of oxygen at temperatures up to 7000 K. This PES is based on *ab-initio* calculations that are interpreted as a combination of van der Waals and electrostatic interaction terms. Unfortunately, the dataset reported in Ref.[37] is incomplete and, thus, a master equation simulation still can not be performed.

An analytical fit to the global *ab-initio* PES of triplet N_2O_2 was recently published by Truhlar's group.[29] This PES was obtained by multi-state complete-active space second-order perturbation theory and was specifically designed to describe collisions at high kinetic energies. Most of the multireference calculations of electron correlation energy were conducted in the range of potential energies between 100 and 350 kcal/mole (76% of the total 54,889 data points). It is worth to note that the long-range forces are not described correctly in this PES, thus it may not be suitable for low energy collisions.

The results section is organized as follows. First, RCs of VV and VT energy transfer for vibrationally excited oxygen and nitrogen are presented for temperatures of 8000, 10,000 and 15,000 K. The QCT transition RCs with vibration-translation energy transfer are compared to the results of the Forced Harmonic Oscillator model.[39] The RCs of monoquantum deactivation of oxygen in VT and VV processes are compared side-by-side. Monoquantum and multiquantum VT RCs with Δv up to 3 are presented as well. In the second part of the result section, the relaxation time of oxygen and nitrogen in collisions with another molecular species is derived from the master equation analysis. Special attention is paid to the influence of monoquantum and multiquantum processes on the magnitude of relaxation times.

A. Full state-resolved results

The simulation of heat bath conditions by means of a master equation requires a complete set of transitions RCs for all possible combinations of initial and final states of target and projectile species. An assumption of trans-rotational equilibrium allows a significant reduction of the database, however, the number of possible transitions between vibrational states remains large. Moreover, the rate of energy exchange between translational and rotational modes becomes comparable to that between translational and vibrational modes at high temperatures, which leads to a certain degree of trans-rotational nonequilibrium. As the first step, the present work assumes trans-rotational equilibrium. Calculations have been conducted for selected vibrational states of oxygen and nitrogen, and the missing RCs are interpolated using the QCT data. Namely, the $O_2(v)$ RCs with v chosen from $\Omega_v = \{0, 1, 2, 5, 10, 15, 20, 25, 30, 31, 32, 33, 34, 35\}$ and for $N_2(w)$ with w chosen from $\Omega_w = \{0, 1, 2, 5, 10, 15, 20, 25, 30, 35, 40, 45, 50, 51, 52, 53\}$ are obtained by the QCT method.

It will be shown later that the bound-bound RCs demonstrate a complex dependence on initial vibrational state of reactants. This is due to the opening of other channels of reaction, such as exchange and dissociation, as well as due to the resonance in transitions with a small vibrational energy defect. For this reason, a global form of such dependence for bound-bound transition RCs is not derived. Instead, a liner interpolation of RCs is applied with the initial vibrational energy of reactant as an independent variable. First, the RCs are interpolated for all O_2 initial vibrational states $v^\star$ at N_2 initial vibrational w from Ω_w:

$$K\left(v^\star, w \to v', w'\right) = \frac{e_v^\star - e_v^L}{e_v^R - e_v^L} K\left(v^R, w \to v', w'\right) + \frac{e_v^R - e_v^\star}{e_v^R - e_v^L} K\left(v^L, w \to v', w'\right), \tag{6}$$

where indices R and L correspond to the vibrational quantum numbers from Ω_v that have higher and lower vibrational energy than the state $v^\star$. No interpolation is required for the first three and for the last five vibrational states of oxygen since the QCT calculations are performed for those v. This is done in order to accurately resolve the relaxation times, average temperature of the gas and dissociation processes. Following this procedure, RCs are evaluated for all initial v and for w from Ω_w. Now, a similar algorithm is applied to interpolate RCs for all initial w. The following equation completes the interpolation procedure:

$$K\left(v, w^\star \to v', w'\right) = \frac{e_w^\star - e_w^L}{e_w^R - e_w^L} K\left(v, w^R \to v', w'\right) + \frac{e_w^R - e_w^\star}{e_w^R - e_w^L} K\left(v, w^L \to v', w'\right). \tag{7}$$

The interpolation procedure, given by Eqs. (6) and (7), introduces some uncertainty in the reaction rate coefficients. In an attempt to quantify this uncertainty, the rate of monoquantum deactivation of oxygen by N_2 is computed in two different manners. The first approach considers collisions of $O_2(v = 1)$ with $N_2(w)$, where w is sampled at T_v=T in the range between 4000 and 15,000 K. By following the described procedure,

the rate of monoquantum deactivation of oxygen, $K_{1\to0}$ is obtained as follows

$$K_{1\to0} = \frac{\sum_w \sum_{w'} K_{v=1,w\to v'=0,w'} exp(-e_w/kT)}{\sum_w exp(-e_w/kT)}. \tag{8}$$

The corresponding relaxation time can be computed using the two-state model, where the relaxation is governed entirely by the monoquantum deactivation from the first excited state, including for the depopulation of v'=0 due to the reverse reaction:

$$p\tau_{1\to0} = \frac{k_B T}{K_{1\to0} - K_{0\to1}}. \tag{9}$$

Equation (9) is used in the present paper to estimate the relaxation time of oxygen and nitrogen. For the latter, the summation in Eq. (8) over w and w' is replaced with the summation over v and v'.

The second approach assumes collisions of $O_2\,(v=1)$ with all possible initial vibrational states of projectile, $N_2\,(w)$ and most frequent final states of projectile $N_2\,(w')$. Since this step presents a computational challenge, collisions are considered only with selected w, and the rest of the rate coefficients are obtained via interpolation on the vibrational energy scale of N_2. This approach, in theory, leads to exactly the same rate of O_2 deactivation, however, it will provide a complete set of rate coefficients that can be implemented in the master equation simulations.

The comparison of $K_{1\to0}$ for temperatures 8000, 10000 and 15000 K, obtained via the two different approaches is shown in Fig. 1. Additionally, the relaxation time of oxygen, computed using Eq. (9), is shown by a line with circular symbols. The experimental data by Losev and Generalov[40] is shown by the filled symbols. One can see a good agreement between the sampling and interpolation approaches. This shows the adequacy of the state-resolved approach at least for low lying vibrational states. Additionally, the QCT rate of monoquantum deactivation provides a satisfactory agreement with the experimental data. This matter will be discussed in details in the following section.

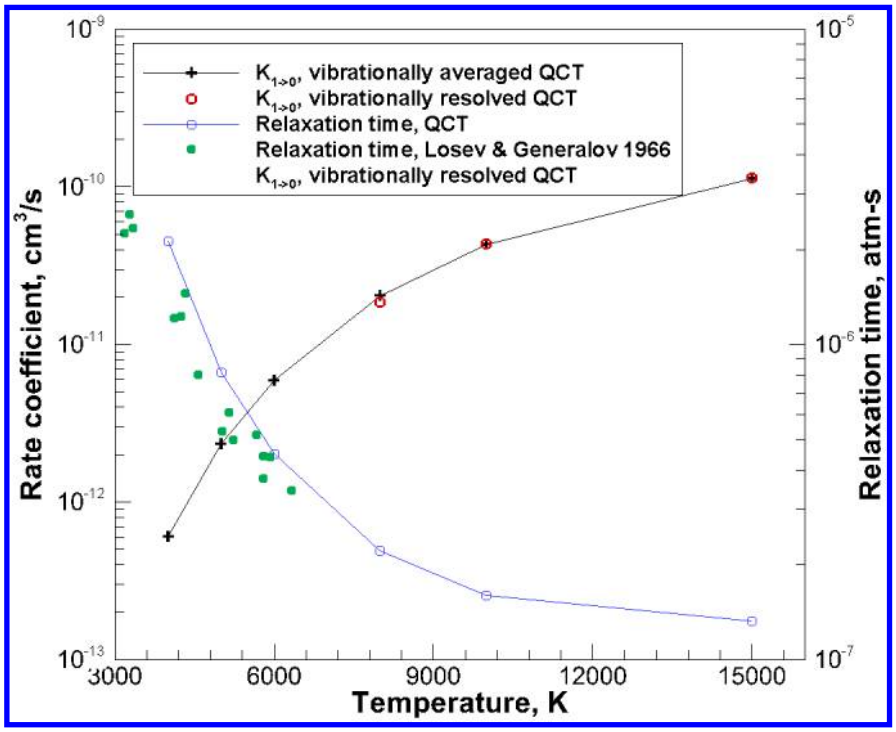

Fig. 1. Monoquantum deactivation rate of oxygen and corresponding relaxation time

B. VT and VV energy transfer

In the present paper, the following types of reactions with the VT vibrational energy transfer are considered:

$$O_2(v) + N_2(w) \rightarrow O_2(v - \Delta v) + N_2(w), \ \Delta v = 1...6 \tag{10}$$

$$O_2(v) + N_2(w) \rightarrow O_2(v) + N_2(w - \Delta w), \ \Delta w = 1...6 \tag{11}$$

Vibration-vibration energy transfer is investigated by computing the rates of the following transitions:

$$O_2(v) + N_2(w) \rightarrow O_2(v - \Delta v) + N_2(w + \Delta w), \ \Delta v = 1...6, \Delta w = 1...3 \tag{12}$$

$$O_2(v) + N_2(w) \rightarrow O_2(v + \Delta v) + N_2(w - \Delta w), \ \Delta v = 1...3, \Delta w = 1...6 \tag{13}$$

$$O_2(v) + N_2(w) \rightarrow O_2(v - \Delta v) + N_2(w - \Delta w), \ \Delta v = 1...5, \Delta w = 1, 2 \tag{14}$$

$$O_2(v) + N_2(w) \rightarrow O_2(v - \Delta v) + N_2(w - \Delta w), \ \Delta v = 1, 2, \Delta w = 1...5 \tag{15}$$

Equation (12) describes the deactivation of oxygen with a simultaneous vibrational activation of nitrogen. Equation (13) describes the opposite transfer of vibration energy, i.e. from nitrogen to oxygen. Equations (14) and (15) describe the simultaneous vibrational deactivation of oxygen and nitrogen. While such energy transfer is less probable than the processes, given by Eqs. (12)-(13), the conditions, considered in the present paper, make these transitions possible.

A principle of detailed balance should be imposed on Eqs. (10) - 15. Because the interpolation routine, given by Eqs. (6) - (7), provides a full set of vibrationally-resolved rate coefficients, it is possible to enforce the principle of detailed balance between specific vibrational levels of target and projectile species. For example, the rate coefficient of a reaction, reverse to the transition $(v, w \rightarrow v', w')$ is calculated as

$$K(v', w' \rightarrow v, w) = K(v, w \rightarrow v', w) Q(v, w, v', w')$$

with $Q(v, w, v', w')$ given by Eq. (16).

$$Q(v, w, v', w') = \frac{\sum_{j=1}^{N_v} g_{v,j}(2j+1) exp(-e_{v,j}/k_B T) \sum_{j=1}^{N_w} g_{w,j}(2j+1) exp(-e_{w,j}/k_B T)}{\sum_{j=1}^{N_{v'}} g_{v',j}(2j+1) exp(-e_{v',j}/k_B T) \sum_{j=1}^{N_{w'}} g_{w',j}(2j+1) exp(-e_{w',j}/k_B T)}, \tag{16}$$

where $e_{v,j}$ and $e_{w,j}$ are the rovibrational energy of $O_2(v, j)$ and $N_2(w, j)$ states, respectively. Interpolated and original QCT rate coefficients of VT transitions leading to O_2 vibrational deactivation are shown in Fig. 2 with thick solid, dashed and dashed dotted lines for temperatures of 8000, 10,000 and 15,000 K, respectively. Thin dashed lines correspond to the monoquantum vibrational activation of nitrogen with oxygen undergoing the same transition as given by thick lines. Symbols of different color represent the original QCT data at different temperatures, while the lines describe the interpolated data.

First of all, the interpolated data for VT transitions aligns exactly with the original QCT data, while some QCT RCs of VV transitions show small deviation from the interpolated results. This is due to the fact that some transitions can be endothermic, and, even if they are captured by the QCT method, the rates of such transitions should be computed using the principle of detailed balance rather than using the original QCT data. Because of the finite size of a batch, used in simulations, the QCT data has a nonzero statistical uncertainty, with the endothermic transitions being resolved less accurately than the exothermic transitions. However, such discrepancy, in theory, should vanish at high temperatures. This is indeed observed for the QCT and interpolated rates in Fig. 2.

The magnitude of both the VV and VT rate coefficients increases with temperature. The VV energy transfer shows a lower sensitivity to temperature and a higher sensitivity to the initial vibrational energy of nitrogen, compared to the VT energy transfer. The VT rate coefficients demonstrate a significant decrease towards the end of the N_2 vibrational ladder due to the opening of the dissociation channel. The difference in VT rate coefficients for different temperatures becomes smaller for vibrationally excited oxygen due to the anharmonicity.

The VV RCs are significantly smaller than the VT RCs when oxygen collides with $N_2(w)$ in a low vibrational state w. This is a quite interesting observation, since the vibrational energy defect in such VV transitions is smaller than in the VT transition. As the vibrational energy initially stored in nitrogen

increases, the rate of VV reaction increases as well, reaching a maximum at around 6 eV for deactivation of oxygen in the first excited vibrational state and shifting to 8.5 eV for highly excited oxygen. This behavior is explained by the effect of anharmonicity, that causes the resonance of vibrational energy transfer.

Comparison of QCT VT RCs with the results of the FHO model is shown in Figs. 3 and 4. The QCT results are shown by solid lines and the FHO rates are given by dashed lines. Rate coefficients are computed for the deactivation of target species, i.e. O_2 in Fig. 3 and N_2 in Fig. 4, by one, two and three vibrational quanta. To make a meaningful comparison with the FHO model, the QCT rate coefficients are averaged according to the Boltzmann distribution of initial vibrational states of a target molecule.

The FHO rates of monoquantum deactivation of oxygen show a satisfactory agreement with the results of the QCT simulation. For low vibrational states, the agreement is less successful. The FHO model overestimates the QCT data with the maximal difference of two times. The agreement improves as the spacing between vibrational state decreases. A similar observation can be made for the rate coefficients of N_2 monoquantum deactivation.

The analysis of VT rate coefficients with multiquantum vibrational jumps leads to the conclusion that the agreement between the FHO and QCT data becomes worse for transitions with a large change of vibrational energy. For two- and three-quantum jumps, the FHO model produces rate coefficients that can be one order of magnitude higher than the QCT data. At the considered temperatures, the magnitude of multiquantum jumps is comparable to that of single quantum transitions, especially for vibrational states with a large degree of anharmonicity. This observation should be taken into account when constructing a kinetic model of vibrationally hot gas flows in a cold environment.

C. Master equation simulation

As the first step, thermal relaxation of O_2 and N_2 is considered by artificially excluding the dissociation reactions and formation of nitric oxide from the kinetic scheme. This means that only VT and VV transitions are considered when simulating the ideal heat bath conditions. In the present work, the heat bath contains two molecular species at a constant translational temperature of 8000, 10,000 and 15,000 K. Molar ratio of O_2 and N_2 is set to 1:4 with the total number density equal to 5×10^{18} cm^{-3}.

There is some uncertainty in specifying the initial thermal conditions. Most of master equation simulations assume a vibrationally cold mixture, i.e. the initial internal temperatures of both species are set to 100 K. Additional numerical experiments assume a completely thermalized vibrational ladder of nitrogen in order to estimate the effect on O_2 relaxation time. Results of these calculations are shown in Fig. 5.

Figure 5(a) presents the relaxation time of oxygen computed via the e-folding method from master equation simulations together with the relaxation time derived from the rate of monoquantum deactivation, shown by triangular and square symbols, respectively. The experimental data by Generalov and Losev[40] and the empirical equation by Millikan and White[41] are shown by circular symbols and curves, with the dashed line designating the Park correction[42] applied to the Millikan and White data.

The master equation results are presented by two datasets of rate coefficients. The first set contains transitions with a maximum change of vibrational quantum number of 5, while the second dataset includes transitions with vibrational jumps of up to 6. These two datasets are generated to verify the convergence of the solution of the master equation. Using the second dataset of rates, the system of master equations is solved for the initial temperature of nitrogen set to the equilibrium conditions.

The O_2 relaxation time derived from $K_{1\to0}$ RC describes the experimental data quite accurately at temperatures below T=6500 K, while the Millikan and White relaxation time lies slightly below the measurements and the $p\tau_{1\to0}$ curve. At a temperature of 10,000 K, the QCT $K_{1\to0}$ relaxation time is nearly equal to the master equation result. This indicates that the relaxation at these conditions is governed by the energy exchange between low lying energy states. The monoquantum transitions possibly play a limiting role here. At temperature of 8000K, the master equation approach produces a slightly higher O_2 relaxation time, which can be attributed to the statistical uncertainty of the QCT rates. If transition rates are insufficiently resolved due to the limiting size of a trajectory batch, this may cause an increase in the relaxation time.

The extended set of rates leads to a subtle decrease of relaxation time, with the most pronounced effect at the translational temperature of 15,000 K. It can be concluded that the present dataset of rate coefficients provide a converged solution in the sense of a number of resolved VT and VV energy transfer channels. The relaxation of oxygen in the heat bath of completely thermalized nitrogen does not change the O_2 relaxation time significantly as well. Time resolved populations of selected vibrational states at T=15,000K are shown in Fig. 6. The population given by the system of master equations is given by solid lines and filled symbols,

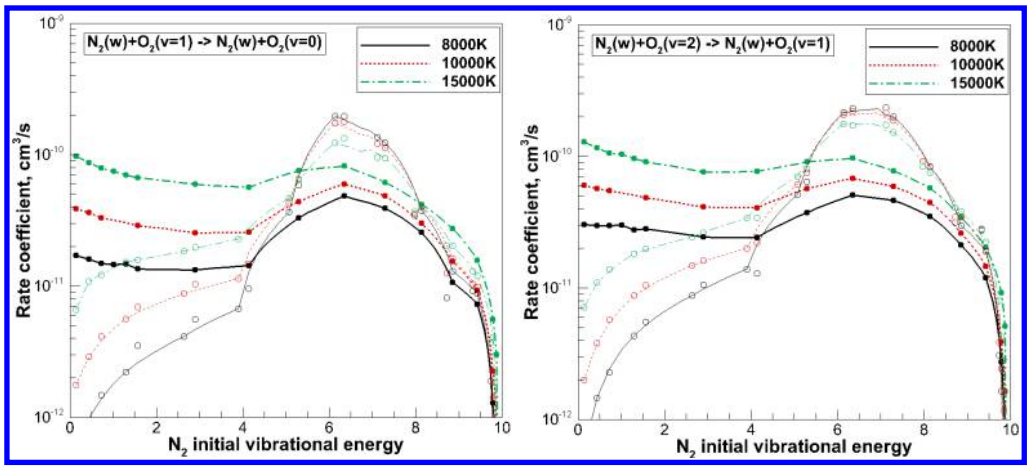

(a) v=1 (b) v=2

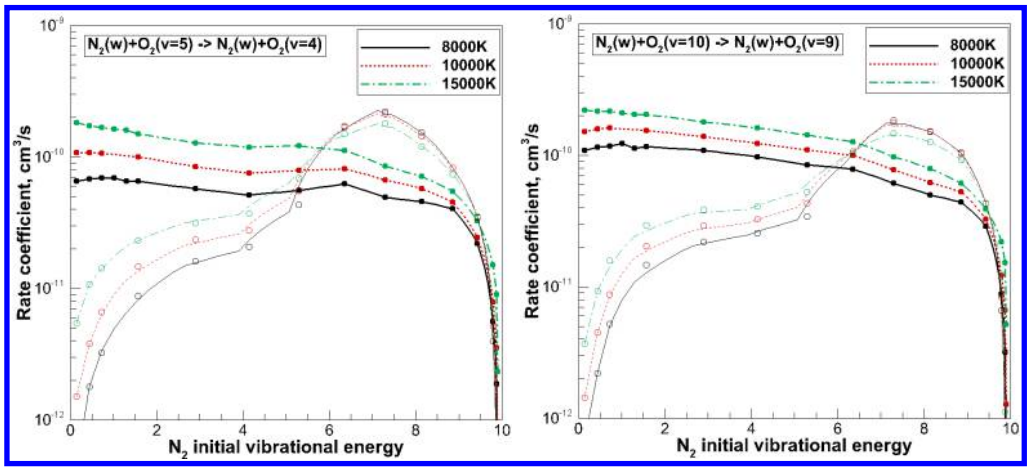

(c) v=5 (d) v=10

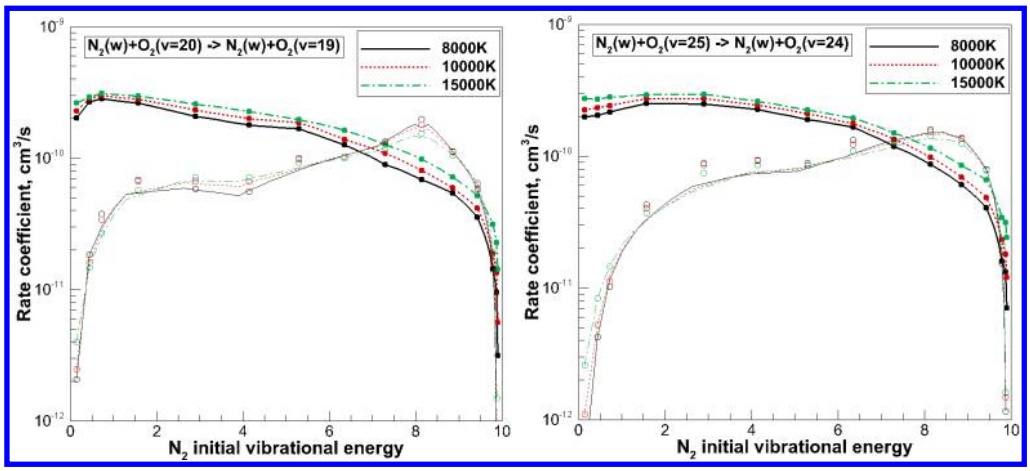

(e) v=20 (f) v=25

Fig. 2. Rate coefficients of vibration-translational energy transfer in reactions $\mathbf{N}_2\,(w) + \mathbf{O}_2\,(v) \rightarrow \mathbf{N}_2\,(w) + \mathbf{O}_2\,(v-1)$ and $\mathbf{N}_2\,(w) + \mathbf{O}_2\,(v) \rightarrow \mathbf{N}_2\,(w+1) + \mathbf{O}_2\,(v-1)$

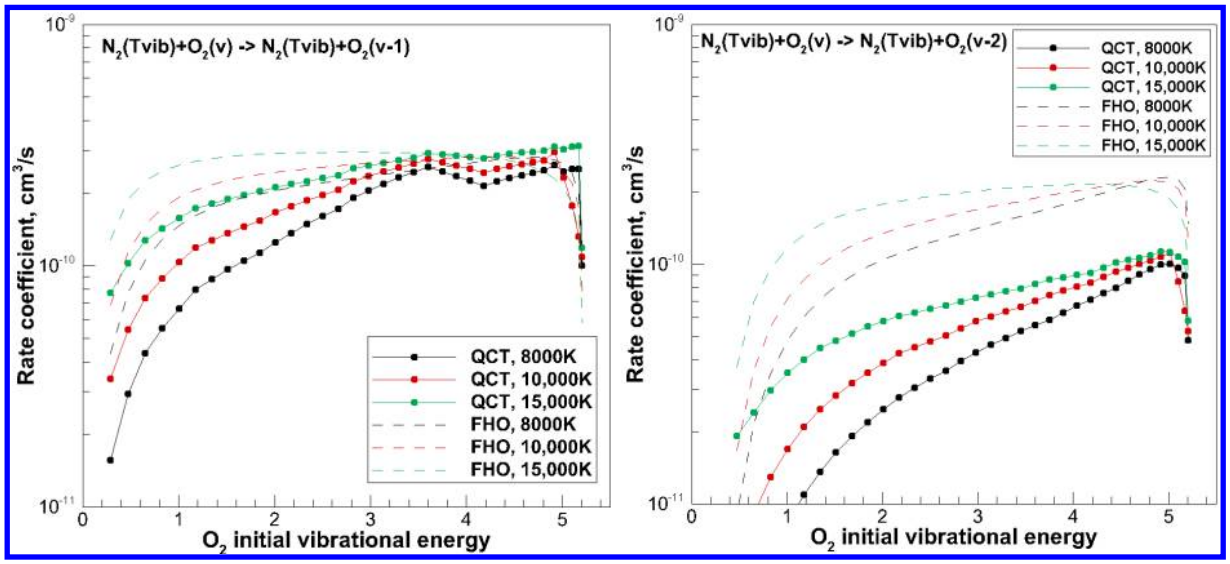

(a) Δv=1

(b) Δv=2

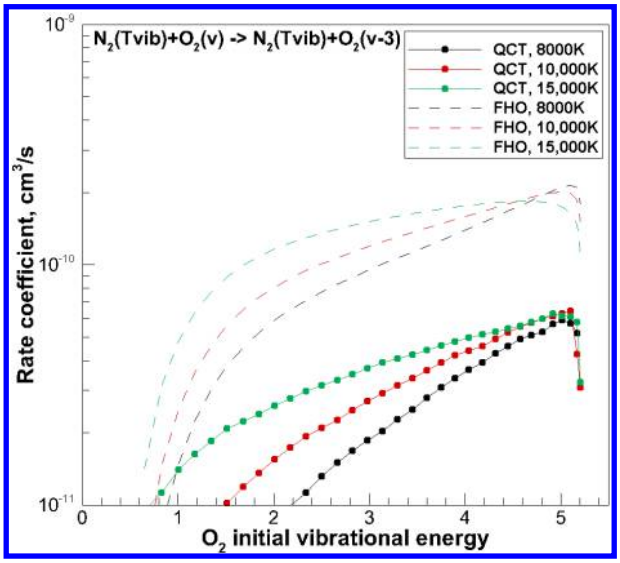

(c) Δv=3

Fig. 3. Rate coefficients of $N_2 + O_2(v) \rightarrow N_2 + O_2(v - \Delta v)$ reaction. Initial vibrational state of nitrogen is sampled at given temperature

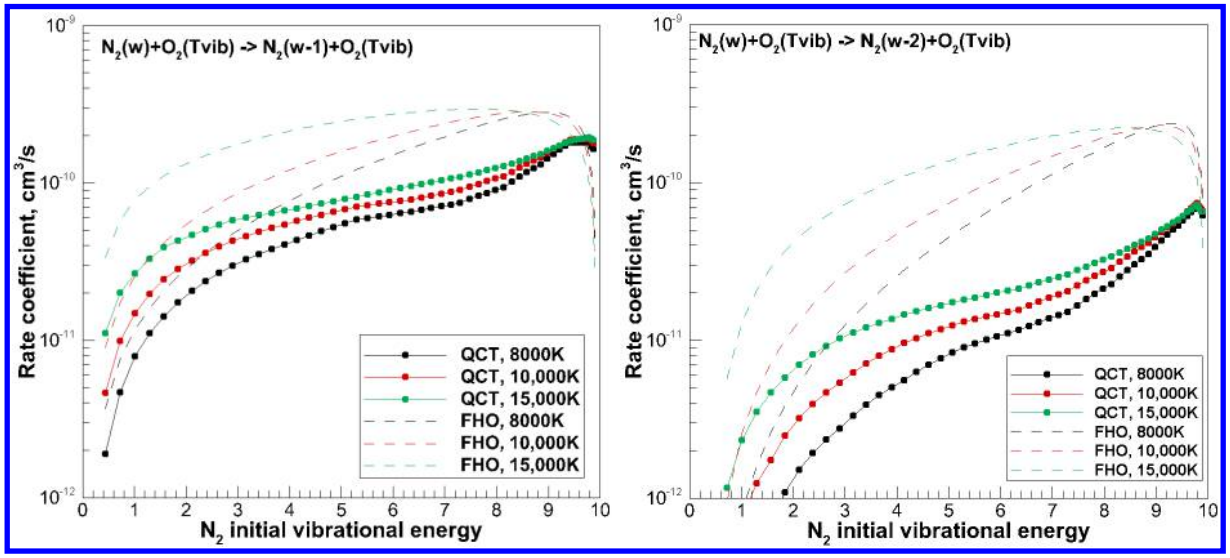

(a) Δw=1 (b) Δw=2

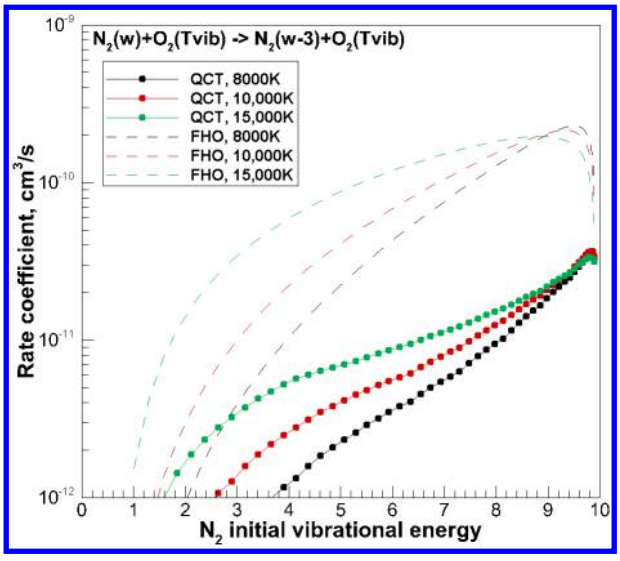

(c) Δw=3

Fig. 4. Rate coefficients of $N_2(w) + O_2 \rightarrow N_2(w - \Delta w) + O_2$ reaction. Initial vibrational state of oxygen is sampled at given temperature

where the former describes the results obtained with the reduced set and the latter is generated with the extended set of transitions rates. Empty symbols correspond to the Boltzmann population of vibrational states at a given vibrational temperature. The extended set of transitions rates leads to an insignificant increase of populations of excited states. This is due to the large number of possible channels of relaxation due to the small spacing of vibrational energy states.

The relaxation time of nitrogen in a heat bath of oxygen is shown in Fig. 5(b). Relaxation times, derived from the $K_{1\to0}$ RC and from a solution of the master equations show close agreement with each other and with the empirical relation by Millikan and White at temperatures of 8000 and 10,000K. At higher translational temperature, the master equation relaxation time is 20 % lower than the $K_{1\to0}$ relaxation time and is in disagreement with the MW relaxation time. Overall, the magnitudes of relaxation times, derived from a simple two-state approach and from the solution of master equations, show a close agreement for both O_2 and N_2 species at the considered temperatures.

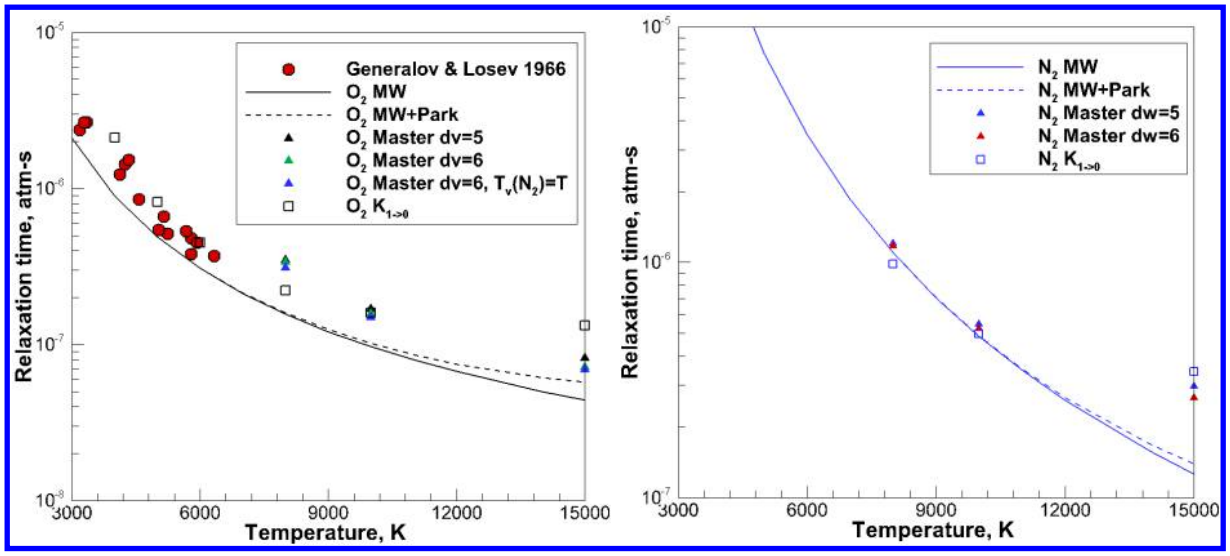

(a) O_2 in collisions with N_2 (b) N_2 in collisions with O_2

Fig. 5. Relaxation times

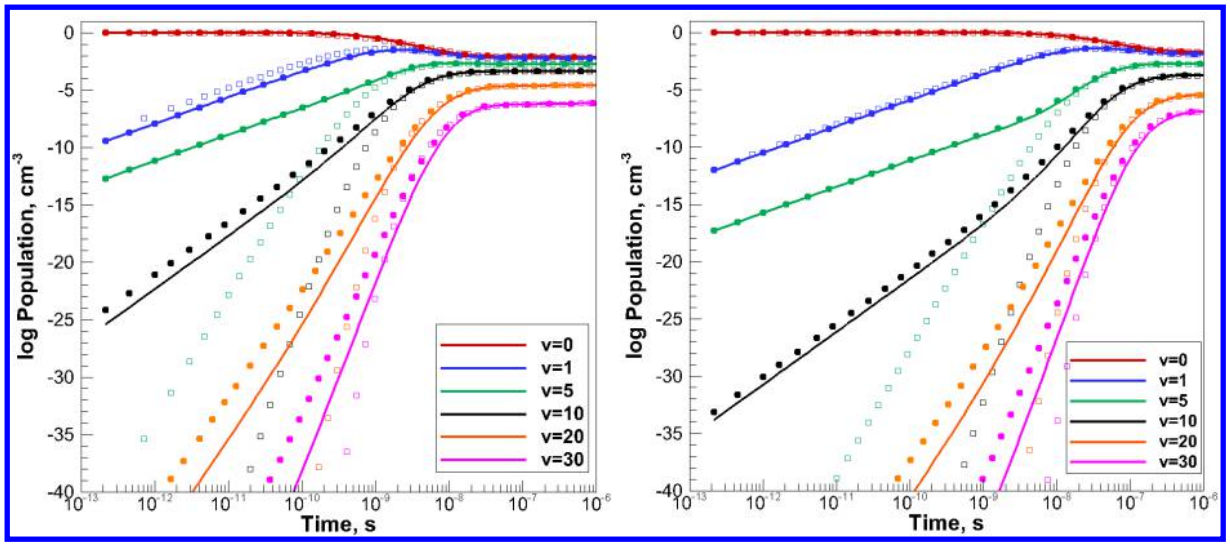

(a) Population of O_2 vibrational ladder (b) Population of N_2 vibrational ladder

Fig. 6. State-resolved populations at T=15,000K

In order to explain the insignificant difference in derived relaxation times, the removal rate of vibrational

energy from a specific energy state of oxygen, v, is considered. The removal rate coefficient, $K_{v,rem}$, is a simple algebraic sum of all bound-bound transition rate coefficients with a final vibrational state $v' \neq v$. In the case when a projectile particle is an atom, calculation of $K_{v,rem}$ is straightforward. In the case of molecule-molecule collision, an additional summation is performed over all final vibrational states of the projectile, w' and the result is averaged over the initial state of projectile, w, using the Boltzmann distribution. By comparing the total removal RC with the RC of monoquantum deactivation, one may judge about the importance of the latter process on the overall relaxation mechanism.

The vibrationally resolved rates in collisions of O_2 with Ar and O have been generated previously.[43] The removal and monoquantum deactivation RCs for these species are shown in Fig. 7(a) and 7(b) at temperatures of 8000, 10000 and 15000 K. The present kinetic data for O_2 in collisions with an N_2 molecule is shown in Fig. 7(c). Solid lines correspond to the $K_{v,rem}$ RC, the dashed lines designate $K_{v\to v-1}$ RC. Symbols show the ratio of $K_{v,rem}$ and $K_{v\to v-1}$.

While the absolute value of a removal RC is not important, the ratio of $K_{v,rem}$ and $K_{1\to 0}$ can explain the deviation of relaxation time derived from the system of master equations from the relaxation time obtained from the $K_{1\to 0}$ RC. For a chemically reactive system, such as O_2–O, this ratio is approximately 0.3 for low lying vibrational states. It quickly decreases to 0.1 for excited vibrational states, indicating the abundance of channels for the removal of vibrational energy in O_2–O collisions. Similar behavior of $K_{v,rem}$ and $K_{v\to v-1}$ ratio is observed for O_2–Ar, although the minimum of the ratio is not as small as for O_2–O.

For O_2–N_2 collisions, the ratio of $K_{v,rem}$ and $K_{v\to v-1}$ rate coefficients remains nearly constant for almost the entire vibrational ladder. The ratio is higher at lower translational temperature, indicating the importance of monoquantum transitions at these conditions. A large contribution of monoquantum deactivation in O_2–N_2 collisions may serve as an explanation of insignificant differences in relaxation times, derived from the $K_{1\to 0}$ rate and from the solution of master equations. A similar situation is observed for nitrogen relaxation in collisions with O_2, as shown in Fig. 7(d).

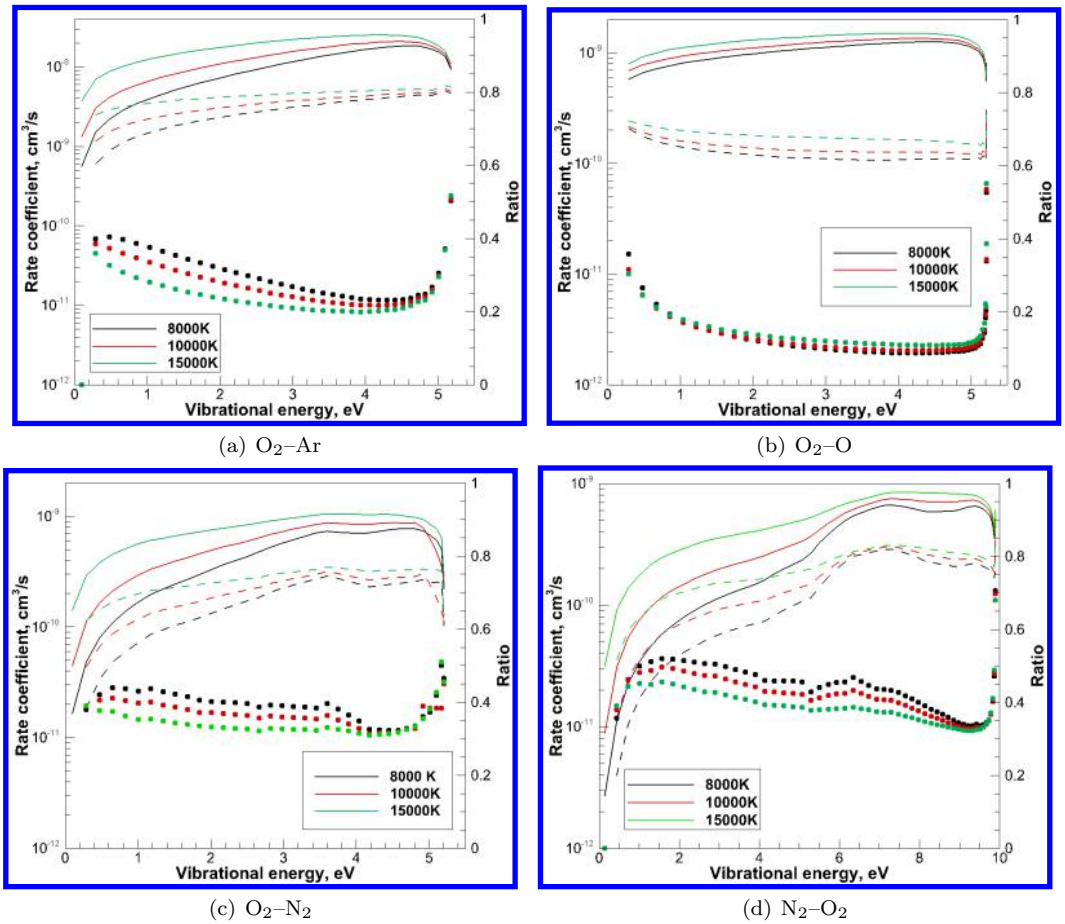

(a) O_2–Ar (b) O_2–O

(c) O_2–N_2 (d) N_2–O_2

Fig. 7. Rate coefficients of removal and monoquantum deactivation of vibrational energy for different species

The master equation approach provides a convenient tool for the study of the VV energy transfer. The variation of vibrational temperature with time for both molecular species is shown in Fig. 8. The solution is obtained with the VV transitions being artificially excluded from the database of rates as well as using a complete set of rates. As follows from Fig. 8, the VV energy transfer has a pronounced effect on the vibrational temperature of oxygen only at the late stage of relaxation. This leads to the conclusion that the O_2 relaxation time, shown in Fig. 5(a), is governed mostly by the VT energy transfer. However, the VV energy transfer significantly delays a complete thermalization of the O_2 vibrational ladder. In fact, during the active VV energy exchange between vibrationally hot oxygen and vibrationally cold nitrogen, the O_2 vibrational temperature remains at the level of approximately $0.9\times T$. The VV energy transfer significantly enhances thermalization of nitrogen, and this effect is most pronounced at T=8000K.

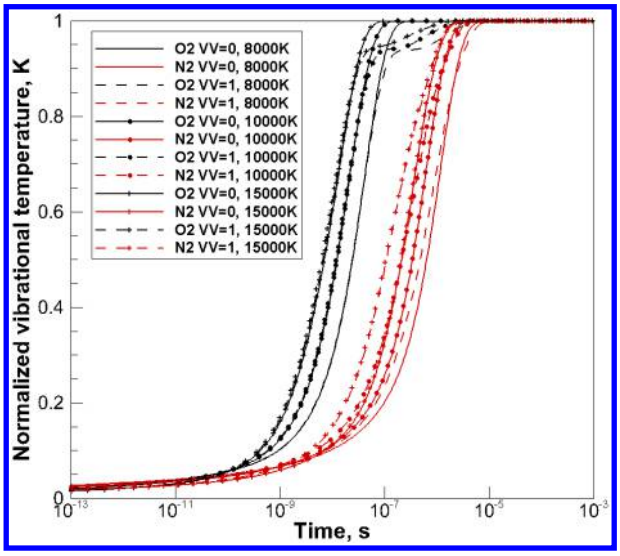

Fig. 8. Variation of O_2 and N_2 vibrational temperature considering only VT and a full set of VT and VV transitions

IV. Conclusion

Vibrational energy transfer in O_2–N_2 collisions is studied by means of the QCT method and the system of master equations. The rate coefficients of vibrational-translation and vibration-vibration energy transfer are generated at typical conditions observed in hypersonics flows with a translational temperature of 8000, 10,000 and 15,000 K.

The analysis of bound-bound rate coefficients indicates the importance of vibration-translation energy transfer for the relaxation of low lying vibrational states. The magnitude of VT rate coefficients does not change significantly with respect to the initial energy of a projectile particle. The magnitude of VV rate coefficients exhibits a more complicated behavior. The vibration-vibration energy transfer is most efficient in reactions with a minimal vibrational energy defect. For this reason, the peak of VV rate coefficients occurs in collisions with a vibrationally excited projectile and shifts towards its higher vibration states.

Relaxation times of nitrogen and oxygen are derived from a simple analysis of a two-state system and from a solution of master equations. Comparison of oxygen relaxation time with the experimental data revealed good agreement at temperatures below 6500 K. Overall, O_2 and N_2 master equation relaxation times show close agreement with the relaxation time, derived from the rate of monoquantum deactivation. The deviation of master equation relaxation time from $p\tau_{1\to 0}$ is more pronounced at high temperatures, however even at T=15,000K the difference is not more than 20 %. These findings are somewhat different from what was previously obtained by means of master equations for molecule-atom systems. The insignificant differences between two derived relaxation times can be partially explained by the chemically inertial nature of the O_2–N_2 interaction. Comparison of the RC of monoquantum deactivation with the RC of total energy removal indicates that the ratio of these RCs for O_2–N_2 is at least two times larger than for the molecule-atom systems. This ratio is particularly low for a chemically reactive system, such as O_2–O.

Acknowledgment

The authors gratefully acknowledge funding for this work through Air Force Office of Scientific Research Grant FA9550-16-1-0291.

References

[1]A. Varandas and A. Pais, "Double many-body expansion potential energy surface for $O_4(^3A)$, dynamics of the $O(^3P)+O_3(^1A_1)$ reaction, and second virial coefficients of molecular oxygen," in *Theoretical and Computational Models for Organic Chemistry*, pp. 55–78, Springer, 1991.

[2]G. D. Billing and R. Kolesnick, "Vibrational relaxation of oxygen. state to state rate constants," *Chemical Physics Letters*, vol. 200, no. 4, pp. 382–386, 1992.

[3]V. Aquilanti, M. Bartolomei, E. Carmona-Novillo, and F. Pirani, "The asymmetric dimer N_2–O_2: characterization of the potential energy surface and quantum mechanical calculation of rotovibrational levels," *Journal of Chemical Physics*, vol. 118, no. 5, pp. 2214–2222, 2003.

[4]R. Schinke, S. Y. Grebenshchikov, M. Ivanov, and P. Fleurat-Lessard, "Dynamical studies of the ozone isotope effect: A status report," *Annu. Rev. Phys. Chem.*, vol. 57, pp. 625–661, 2006.

[5]J. D. Bender, P. Valentini, I. Nompelis, T. Schwartzentruber, and G. V. Candler, "Characterization of vibrational and rotational energy transfer in N_2+N_2 dissociative collisions using the quasiclassical trajectory method," 45th AIAA Thermophysics Conference, AIAA paper 2015-3253, June 2015.

[6]M. Panesi, R. L. Jaffe, D. W. Schwenke, and T. E. Magin, "Rovibrational internal energy transfer and dissociation of $N_2(^1\Sigma_g^+)$- $N(^4S_u)$ system in hypersonic flows," *Journal of Chemical Physics*, vol. 138, no. 4, p. 044312, 2013.

[7]F. Esposito, M. Capitelli, and C. Gorse, "Quasi-classical dynamics and vibrational kinetics of N+$N_2(v)$ system," *Chemical Physics*, vol. 257, no. 2, pp. 193–202, 2000.

[8]J. G. Kim and I. D. Boyd, "State-resolved master equation analysis of thermochemical nonequilibrium of nitrogen," *Chemical Physics*, vol. 415, pp. 237–246, 2013.

[9]R. Fiévet, S. J. Voelkel, V. Raman, and P. L. Varghese, "Numerical investigation of vibrational relaxation coupling with turbulent mixing," in *55th AIAA Aerospace Sciences Meeting*, p. 0663, 2017.

[10]D. Bose, G. V. Candler, *et al.*, "Thermal rate constants of the O_2+N → NO+O reaction based on the $^2A'$ and $^4A'$ potential-energy surfaces," *Journal of Chemical Physics*, vol. 107, no. 16, pp. 6136–6145, 1997.

[11]J. W. Duff and R. D. Sharma, "Quasiclassical trajectory study of NO vibrational relaxation by collisions with atomic oxygen," *Journal of the Chemical Society, Faraday Transactions*, vol. 93, no. 16, pp. 2645–2649, 1997.

[12]M. González, R. Valero, and R. Sayós, "Ab initio and quasiclassical trajectory study of the n (2d)+ no (x 2π) o (1d)+ n2 (x 1σg+) reaction on the lowest 1a potential energy surface," *Journal of Chemical Physics*, vol. 113, no. 24, pp. 10983–10998, 2000.

[13]J. C. Castro-Palacio, T. Nagy, R. J. Bemish, and M. Meuwly, "Computational study of collisions between $O(^3P)$ and NO $(^2\Pi)$ at temperatures relevant to the hypersonic flight regime," *The Journal of chemical physics*, vol. 141, no. 16, p. 164319, 2014.

[14]H. Luo, M. Kulakhmetov, and A. Alexeenko, "Ab initio state-specific n2+ o dissociation and exchange modeling for molecular simulations," *The Journal of Chemical Physics*, vol. 146, no. 7, p. 074303, 2017.

[15]K. Yamashita, K. Morokuma, F. Le Quéré, and C. Leforestier, "New ab initio potential surfaces and three-dimensional quantum dynamics for transition state spectroscopy in ozone photodissociation," *Chemical Physics Letters*, vol. 191, no. 6, pp. 515–520, 1992.

[16]R. Siebert, P. Fleurat-Lessard, R. Schinke, M. Bittererová, and S. Farantos, "The vibrational energies of ozone up to the dissociation threshold: Dynamics calculations on an accurate potential energy surface," *Journal of Chemical Physics*, vol. 116, no. 22, p. 9749, 2002.

[17]V. G. Tyuterev, S. Tashkun, P. Jensen, A. Barbe, and T. Cours, "Determination of the effective ground state potential energy function of ozone from high-resolution infrared spectra," *Journal of Molecular Spectroscopy*, vol. 198, no. 1, pp. 57–76, 1999.

[18]A. Varandas and A. Pais, "A realistic double many-body expansion (DMBE) potential energy surface for ground-state O_3 from a multiproperty fit to ab initio calculations, and to experimental spectroscopic, inelastic scattering, and kinetic isotope thermal rate data," *Molecular Physics*, vol. 65, pp. 843–860, Nov 1988.

[19]H. Webster III and E. J. Bair, "Ozone ultraviolet photolysis. IV. O_2+ $O(^3P)$ vibrational energy transfer," *Journal of Chemical Physics*, vol. 56, pp. 6104–6108, 1972.

[20]D. A. Andrienko and I. D. Boyd, "Rovibrational energy transfer and dissociation in O_2–O collisions," *Journal of Chemical Physics*, vol. 144, no. 10, p. 104301, 2016.

[21]F. Esposito, I. Armenise, G. Capitta, and M. Capitelli, "O+O_2 state-to-state vibrational relaxation and dissociation rates based on quasiclassical calculations," *Chemical Physics*, vol. 351, no. 1-3, pp. 91–98, 2008.

[22]C. Coletti and G. D. Billing, "Vibrational energy transfer in molecular oxygen collisions," *Chemical Physics Letters*, vol. 356, no. 1, pp. 14–22, 2002.

[23]G. D. Billing, "VV and VT rates in N_2–O_2 collisions," *Chemical Physics*, vol. 179, no. 3, pp. 463–467, 1994.

[24]H. Park and T. Slanger, "O_2(X,v=8–22) 300 K quenching rate coefficients for O_2 and N_2, and O_2(X) vibrational distribution from 248 nm O_3 photodissociation," *Journal of Chemical Physics*, vol. 100, no. 1, pp. 287–300, 1994.

[25]J. Price, J. Mack, C. Rogaski, and A. Wodtke, "Vibrational-state-specific self-relaxation rate constant. measurements of highly vibrationally excited $O_2(\nu = 19 - 28)$," *Chemical Physics*, vol. 175, no. 1, pp. 83–98, 1993.

[26]A. Varandas, "Are vibrationally excited molecules a clue for the O_3 deficit problem and HO_x dilemma in the middle atmosphere?," *Journal of Physical Chemistry A*, vol. 108, no. 5, pp. 758–769, 2004.

[27]R. Jaffe, D. Schwenke, and G. Chaban, "Vibrational and rotational excitation and dissociation in N_2-N_2 collisions from accurate theoretical calculations," 10th AIAA/ASME Joint Thermophysics and Heat Transfer Conference, AIAA Paper 2010-4517, June 2010.

[28]Y. Paukku, K. R. Yang, Z. Varga, and D. G. Truhlar, "Global ab initio ground-state potential energy surface of N_4," *Journal of Chemical Physics*, vol. 139, no. 4, p. 044309, 2013.

[29]Z. Varga, R. Meana-Pañeda, G. Song, Y. Paukku, and D. G. Truhlar, "Potential energy surface of triplet N_2O_2," *Journal of Chemical Physics*, vol. 144, no. 2, p. 024310, 2016.

[30]K. Koura, "Monte carlo direct simulation of rotational relaxation of diatomic molecules using classical trajectory calculations: Nitrogen shock wave," *Physics of Fluids*, vol. 9, no. 11, pp. 3543–3549, 1997.

[31]G. D. Billing, "Semiclassical theory for diatom-diatom collisions," *Chemical Physics Letters*, vol. 97, no. 2, pp. 188–192, 1983.

[32]L. M. Raff, D. L. Thompson, L. Sims, and R. N. Porter, "Dynamics of the molecular and atomic mechanisms for the hydrogen-iodine exchange reaction," *Journal of Chemical Physics*, vol. 56, no. 12, pp. 5998–6027, 1972.

[33]D. Andrienko and I. D. Boyd, "Investigation of oxygen vibrational relaxation by quasi-classical trajectory method," *Chemical Physics*, vol. 459, pp. 1–13, 2015.

[34]C. Park, "Rotational relaxation of N_2 behind a strong shock wave," *Journal of Thermophysics and Heat Transfer*, vol. 18, no. 4, pp. 527–533, 2004.

[35]M. Quack and J. Troe, "Complex formation in reactive and inelastic scattering: Statistical adiabatic channel model of unimolecular processes III," *Berichte der Bunsengesellschaft für physikalische Chemie*, vol. 79, no. 2, pp. 170–183, 1975.

[36]M. Bartolomei, E. Carmona-Novillo, M. I. Hernández, J. Campos-Martínez, and R. Moszynski, "Global ab initio potential energy surface for the $O_2(^3\Sigma_g^-)$+$N_2(^1\Sigma_g^+)$ interaction. applications to the collisional, spectroscopic, and thermodynamic properties of the complex," *Journal of Physical Chemistry A*, vol. 118, no. 33, pp. 6584–6594, 2014.

[37]E. Garcia, A. Kurnosov, A. Lagana, F. Pirani, M. Bartolomei, and M. Cacciatore, "Efficiency of collisional O_2+N_2 vibrational energy exchange," *Journal of Physical Chemistry B*, 2015.

[38]E. Garcia, F. Pirani, A. Lagana, and C. Martí, "The role of the long-range tail of the potential in o2+ n2 collisional inelastic vibrational energy exchange transfers," *Physical Chemistry Chemical Physics*, 2017.

[39]I. V. Adamovich, S. O. Macheret, J. W. Rich, and C. E. Treanor, "Vibrational relaxation and dissociation behind shock waves. part 1-kinetic rate models.," *AIAA journal*, vol. 33, no. 6, pp. 1064–1069, 1995.

[40]N. Generalov and S. Losev, "Vibrational exitation and decomposition of molecular oxygen and carbon dioxide behind shock waves," *Journal of Quantum Spectroscopy and Radiative Transfer*, vol. 6, pp. 101–125, 1966.

[41]R. C. Millikan and D. R. White, "Systematics of vibrational relaxation," *Journal of Chemical Physics*, vol. 39, no. 12, pp. 3209–3213, 1963.

[42]C. Park, *Nonequilibrium hypersonic aerothermodynamics*. Wiley, 1989.

[43]D. A. Andrienko and I. D. Boyd, "Kinetic models of oxygen thermochemistry based on quasi-classical trajectory analysis," *Journal of Thermophysics and Heat Transfer*, pp. 1–13, 2016.